ARCHIVES OF ELECTRICAL ENGINEERING VOL. 68(2), pp. 341–356 (2019)

DOI 10.24425/aee.2019.128272

Power flow controller based on bipolar direct PWM AC/AC converter operation with active load

JACEK ZBIGNIEW KANIEWSKI

Institute of Electrical Engineering, University of Zielona Gora, Poland
e-mail: j.kaniewski@iee.uz.zgora.pl

(Received: 02.10.2018, revised: 14.01.2019)

Abstract: The uncontrolled power flow in the AC power system caused by renewable energy sources (restless sources, distributed energy sources), dynamic loads, etc., is one of many causes of voltage perturbation, along with others, such as switching effects, faults, and adverse weather conditions. This paper presents a three-phase voltage and power flow controller, based on direct PWM AC/AC converters. The proposed solution is intended to protect sensitive loads against voltage fluctuation and problems with power flow control in an AC power system. In comparison to other solutions, such as DVR, UPFC, the presented solution is based on bipolar matrix choppers and operates without a DC energy storage unit or DC link. The proposed solution is able to compensate 50% voltage sags, in the case of three-phase symmetrical voltage perturbation, and single phase voltage interruptions. Additionally, by means of a voltage phase control with a range of ±60° in each phase, it is possible to control the power flow in an AC power system. The paper presents an operational description, a theoretical analysis based on the averaged state space method and four terminal descriptions, and the experimental test results from a 1 kVA laboratory model operating under active load.

Key words: power flow controller, direct AC/AC converter, matrix chopper, power quality

1. Introduction

The modern electrical power system is being increasingly saturated with distributed energy sources, especially renewable sources such as wind farm and photovoltaic systems, etc. Generated energy from renewable energy sources are strongly dependant on primary energy (wind, sunshine). In consequence, the operation of restless sources can lead to uncontrolled power flows between particularly parts of the electrical AC power system [1, 2]. The uncontrolled power flow and other causes, such as adverse weather conditions, dynamic loads, and switching effects, generate

undesirable end-user effects, such as voltage sags/swells, voltage variations, voltage unbalance, interruptions and flicker effects [3]. To limit and control the power flow in the power system, power flow controllers are installed. Devices such as phase shifters and more advanced as well as various types of unified power flow controllers (UPFCs) are implemented to control power flow [4–10]. The first group is usually based on thyristor converters with transformers and quadrature phase shifters, however such devices have limited properties and a narrow control range [4, 5] or, as in the case of quadrature converters [6], they change the voltage at the connection point. The concept of the UPFC is well known and widely described in the literature and is still being developed [7–11]. Conventional UFPFCs are based on AC/DC/AC converters [7, 8] and contain a DC link with a DC energy storage unit (usually electrolytic capacitor). The principle of operation and classical topology of the UPFC is shown in Fig. 1.

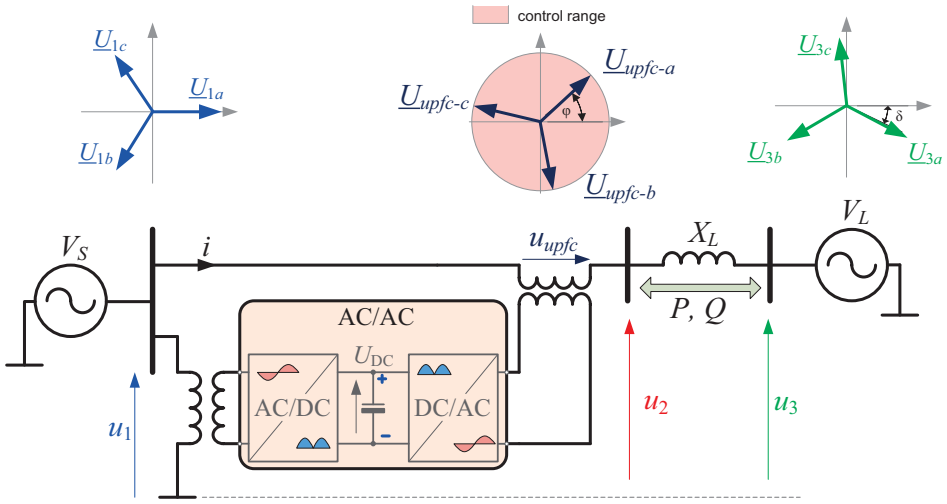

(a)

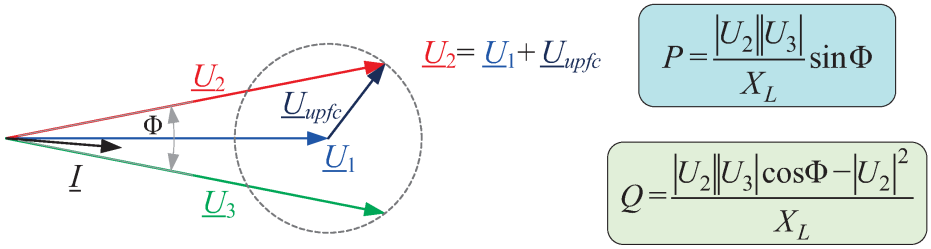

(b)

Fig. 1. Simplified schema of conventional UPFC (a), voltage phasors (b)

The electrolytic capacitor bank is the main factor contributing to their size, and is the most frequently damaged component in operation [12, 13]. An alternative solution to conventional UPFCs employs devices with direct PWM AC/AC converters, without a DC link and electrolytic

capacitor bank [9, 11]. The solutions based on a full matrix converter [9, 10] allow for the power flow control and control of amplitude and voltage phase independently, however they need many bidirectional switches and a complicated and advanced control system. The power flow controller described in [11] uses two bipolar Ćuk B2 matrix-reactance choppers in each phase. This type of AC/AC converter has strongly nonlinear characteristics of voltage gain and an input power factor and a limited useful working area, as well as it is being additionally susceptible to poor matching conditions. This means that the voltage gain depends on load impedance. This paper develops a concept described in [11] by replacement of the matrix-reactance chopper with the other type of direct AC/AC converter – the bipolar matrix chopper (*MC*), which has other properties in comparison to the matrix-reactance chopper. Implementation of this type of bipolar *MC* as a voltage sag/swell compensator is presented in [14, 15]. The simulation test results of the power flow controller with bipolar AC/AC, based on the *MC* and principle of operation are described in [16]. The main advantage of the considered circuit in comparison to e.g. quadrature phase shifters [6] is greater functionality, especially the possibility of simultaneous and independent control of the amplitude and phase of voltage in a wider range. In comparison to a conventional UPFC with AC/DC/AC converters [7, 8] the proposed solution is devoid of an electrolytic capacitor bank, which is the most frequently damaged element. In addition, the used *MC* is self-synchronizing with the AC grid and has just one stage of AC to AC energy convertsion. In comparison to solutions based on a full matrix converter [9, 10], presented solution has a less complicated structure and voltage gain of the used matrix chopper is from 0 to 1 [14, 15], while in the case of a full matrix converter up to 0.866 of source voltage [12]. In comparison to the Ćuk B2 matrix reactance chopper implemented in [11], the used bipolar matrix chopper has linear characteristics, a simpler structure, a wider operating range, a better input power factor across the operating range and lack of susceptibility to matching conditions [14, 15].

This paper extends the research described in [16] by introducing a mathematical model and theoretical analysis in a steady state. The presented solution has the ability to control simultaneously and independently the amplitude and phase of the voltage and to compensate up to 50% of three-phase voltage sag and single-phase voltage interruptions without a DC energy storage unit. These properties, in addition to voltage regulation, allow power flow control in a system with active load. The main aim of this paper is the presentation of the proposed topology of a power flow controller, description of the principle of operation, checking the possibility of bidirectional power flow in a two-source system (active load) and the analysis of the basic properties such as the range of amplitude and phase control of output voltage.

2. Operational description

The schema of the main circuit of the considered three-phase power flow controller is shown in Fig. 2. The considered circuit, as in the case of a conventional topology of the UPFC, is a kind of series device. It contains three power electronic modules (PE I, PE II, PE III) (Fig. 2). Power electronic module PE I operates on line L_1, but is supplied from two other phases – from line L_2, and L_3. Analogously PE II operates on line L_2, but is supplied from lines L_1 and L_3, and PE III operates on line L_3, but is supplied from lines L_1 and L_2 (Fig. 2).

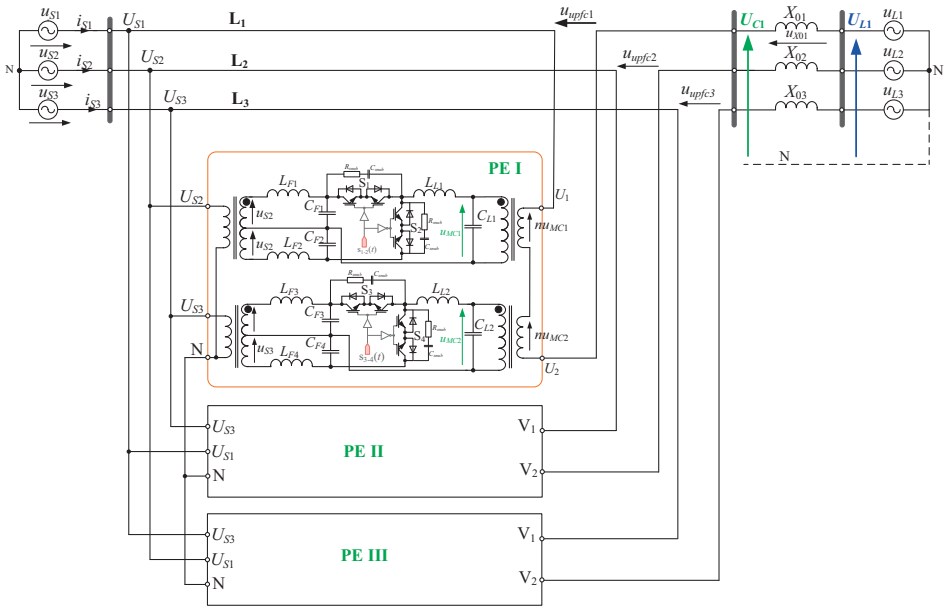

Fig. 2. Simplified schema of proposed three-phase power flow controler

Each of PE units consists of two bipolar AC/AC converters based on a conventional matrix chopper (*MC*1 and *MC*2) (Fig. 3).

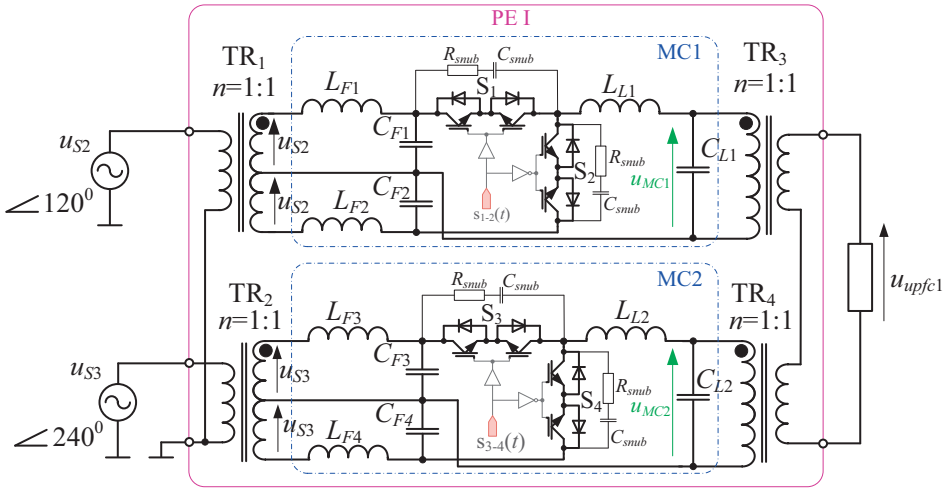

Fig. 3. Schema of a single power electronic modul PE I

With the bipolar converter, it is possible to obtain an output voltage from the "in-phase" or the "anti-phase" in relation to the input voltage and dependant on pulse duty factor D. The bipolar

character of the output voltage can be achieved by implementation of various solutions of AC/AC converters [15], e.g. a full bridge AC/AC converter [16] or a bipolar matrix-reactance chopper [11]. The employed bipolar AC/AC converter needs only two bidirectional switches, S_1 and S_2, but also requires a symmetrical supply voltage source realized by a transformer (TR_1, TR_2) with two symmetrical secondary windings (Fig. 4) [14, 15]. The outputs of both MCs ($MC1$ and $MC2$) are connected to the primary side of transformers TR_3 and TR_4, respectively. The secondary sides of TR_3 and TR_4 are connected in series (Fig. 4). The voltage ratios of TR_3 and TR_4 equal to 1 ($n_{TR3} = n_{TR4} = n = 1$). For obtaining two symmetrical input voltages, two input transformers (TR_1 and TR_2) with two secondary windings are used. The voltage ratios of the input transformers are also equal to 1 ($n_{TR1} = n_{TR2} = n = 1$). The power electronic switches $S_1 - S_4$ are controlled by the classical PWM modulation method, where the modulated signal (triangle) is compared with the modulating signal (constant signal). Each of the two MCs is controlled independently by pulse duty factors D_1 and D_2. The idealized voltage transmittance of a simple MC is defined as (1) [15].

$$\left|\underline{H}_U^{MC}\right| = \left|\frac{\underline{U}_{MC}}{\underline{U}_S}\right| \cong |(2D-1)|, \tag{1}$$

where: $\underline{U}_{MC}$ is the output voltage of the matrix chopper, $\underline{U}_S$ is the input voltage of the matrix chopper, D is the pulse duty factor which is defined as a relation between a switching period and switch S_1 conducting time (T_S/t_{on}). Taking into account (1), the output voltages of $MC1$ and $MC2$ are described as (2) and (3), respectively:

$$\underline{U}_{MC1} = \underline{U}_{S2}\,(2D_1 - 1)\,, \tag{2}$$

$$\underline{U}_{MC2} = \underline{U}_{S3}\,(2D_2 - 1)\,. \tag{3}$$

The output voltage of PE I ($\underline{U}_{upfc1}$) is the sum of the output voltages of matrix choppers $MC1$ and $MC2$ ($\underline{U}_{MC1}$, $\underline{U}_{MC2}$) (5).

$$\underline{U}_{upfc1} = \underline{U}_{MC1} + \underline{U}_{MC2}\,. \tag{4}$$

Describing three-phase source voltages for $\omega t = 0$ as (5), assuming voltage ratios of all transformers as unity then according to (2) and (3) we can easily obtain an output voltage in

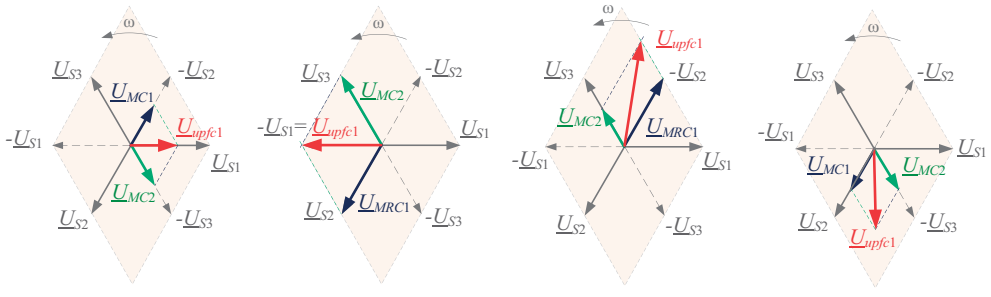

Fig. 4. Exemplary voltage phasors of PE I for conditions: (a) $D_1 = D_2 = 0.25$; (b) $D_1 = D_2 = 1$; (c) $D_1 = 0$, $D_2 = 0.75$; (d) $D_1 = 0.75$, $D_2 = 0.25$

complex form ($\underline{U}_{upfc1}$) for power electronic module PE I (6). In the same way, voltages for other lines ($\underline{U}_{upfc2}$ and $\underline{U}_{upfc3}$) are construed.

$$\underline{U}_{S1} = U_S \cdot e^{j0}, \qquad \underline{U}_{S2} = U_S \cdot e^{j\frac{-2\pi}{3}}, \qquad \underline{U}_{S3} = U_S \cdot e^{j\frac{2\pi}{3}}, \tag{5}$$

$$\underline{U}_{upfc1} = U_S \left(e^{j\frac{-2\pi}{3}} \cdot (2D_1 - 1) + e^{j\frac{2\pi}{3}} \cdot (2D_2 - 1) \right). \tag{6}$$

The exemplary voltage phasors of power electronic module PE I for various conditions, showing the principle of operation, are presented in Fig. 5. According to (6) and as can be seen in Fig. 4, the voltage vector $\underline{U}_{upfc1}$ is constructed from two phasors – $\underline{U}_{MC1}$ and $\underline{U}_{MC2}$.

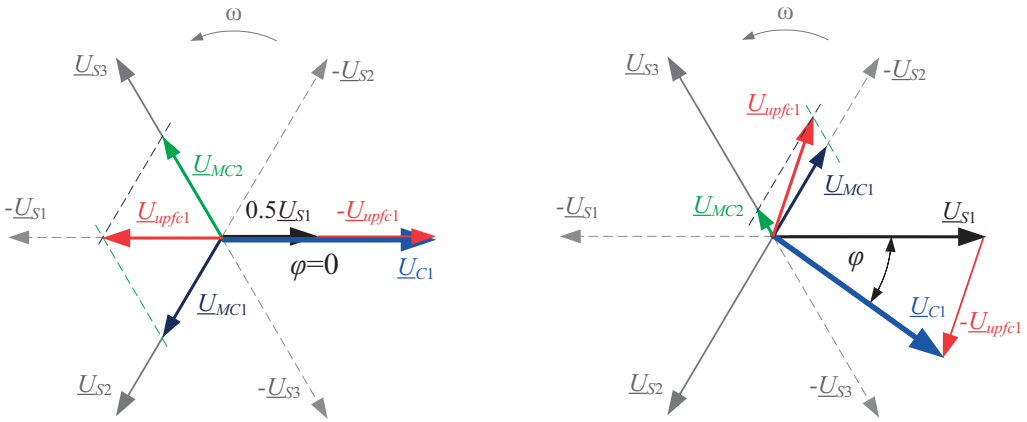

Fig. 5. Exemplary voltage phasors of UPFC circuit for pulse duty factors: (a) $D_1 = D_2 \approx 0.75$; (b) $D_1 \approx 0.2$, $D_2 \approx 0.57$

Because matrix chopper $MC1$ is supplied from line L_2 (by voltage U_{S2}) and has a bipolar character, voltage U_{MC1} could be in-phase or anti-phase in relation to voltage U_{S2}. It is analogous in the case of $MC2$ (see Fig. 2 and 3) supplied from line L_3 (U_{S3}). If pulse duty factors D_1 and D_2 are in the range from 0 to 0.5, voltages $\underline{U}_{MC1}$ and $\underline{U}_{MC2}$ are in anti-phase in relation to input voltages. If pulse duty factors D_1 and D_2 are in the range from 0.5 to 1, voltages $\underline{U}_{MC1}$ and $\underline{U}_{MC2}$ are in-phase in relation to input voltages. In consequence the output voltage of power electronic module PE I ($\underline{U}_{upfc1}$) can be controlled in magnitude and phase independently. If pulse duty factors D_1 and D_2 are equal ($D_1 = D_2$) only the amplitude of the voltage changes (without a change of phase angle) (Fig. 4(a), 4(b)). If pulse duty factors are different ($D_1 \neq D_2$) (Fig. 4(c), 4(d)) then magnitude and phase angle change. The operating area of output voltage PE I ($\underline{U}_{upfc1}$) is indicated by a dashed line (Fig. 4). Voltages U_{C1}, U_{C2} and U_{C3} of the considered UPFC are a sum of source voltages U_{S1}, U_{S2}, U_{S3} and the output voltage of power electronic modules PE I–PE III (U_{upfc1}, U_{upfc2}, U_{upfc3}). Taking into account (5) and (6), voltage $\underline{U}_{C1}$ in complex form for the first phase (line L_1) is described by (7).

$$\underline{U}_{C1} = U_S \cdot e^{j(\omega t)} - U_S \left(e^{j\left(\omega t - \frac{2\pi}{3}\right)} \cdot (2D_1 - 1) + e^{j\left(\omega t + \frac{2\pi}{3}\right)} \cdot (2D_2 - 1) \right). \tag{7}$$

The exemplary voltage phasors in the considered UPFC for condition $D_1 = D_2$ and $D_1 \neq D_2$ are shown in Fig. 5(a) and 5(b), respectively.

In the case when the both pulse duty factors are the same ($D_1 = D_2$) only the amplitude of voltage $\underline{U}_{upfc}$ is controlled (Fig. 5(a)). According to (7), for pulse duty factors $D_1 = D_2 = 0.75$ and assuming a 50% voltage sag of voltage $\underline{U}_{S1}$ (Fig. 5(a)) the amplitude of voltage $\underline{U}_{upfc1} \approx 0.5\underline{U}_{S1}$, and according to (7) voltage $\underline{U}_{C1} \approx \underline{U}_{S1}$. If pulse duty factors D_1 and D_2 are different ($D_1 \neq D_2$), as is visible in Fig. 6(b), both parameters, amplitude and phase of voltage $\underline{U}_{upfc}$ are controlled. For example for pulse duty factors $D_1 = 0.2$, $D_2 = 0.57$ and according to (7) the amplitude of voltage $\underline{U}_{C1}$ is approximately equal to the amplitude of $\underline{U}_{S1}$, but it is shifted in phase by angle $\varphi \approx 40^\circ$ in relation to $\underline{U}_{S1}$ (Fig. 5b).

3. Theoretical analysis

The main properties of the considered power flow controller were analysed on the basis of the averaged state space method (8) and four-terminal description, which is comprehensively and in detail described in [17–19], and implemented in [20].

$$\dot{\bar{\boldsymbol{x}}} \cong \boldsymbol{A}(D)\,\bar{\boldsymbol{x}} + \boldsymbol{B}(D)\,\boldsymbol{u}_S\,, \tag{8}$$

where: $\bar{\boldsymbol{x}}$ is the vector of the averaged variables, $\boldsymbol{A}(D)$ is the averaged state matrix, $\boldsymbol{B}(D)$ is the averaged input matrix [17–20]. On the basis of the averaged state space method (8) and averaged circuit model of bipolar matrix choppers $MC1$ and $MC2$ described in [21], an averaged circuit model of the considered power flow controller is constructed and shown in Fig. 6. For the sake of analysis, the averaged circuit model is divided into four terminal networks.

As we can see in Fig. 6, and as it is already mentioned, the power electronic module PE I operating in the first ($L1$) phase is supplied from two other phases ($L2$ and $L3$). For this reason it is necessary to introduce matrixes of chain parameters to describe phase dependencies in a three-phase system – between operating phase $L1$ and phase $L2$ supplying $MC1$ (9), and between operating phase $L1$ and $L3$ supplying $MC2$ (10). All transformer ratios are assumed as 1:1 ($n_{TR1} = n_{TR2} = n_{TR3} = n_{TR4} = 1$).

$$\underline{\boldsymbol{A}}_{L1-2} = \begin{bmatrix} \dfrac{1}{(-0.5 - j\sqrt{3/2})} & 0 \\ 0 & (-0.5 - j\sqrt{3/2}) \end{bmatrix}, \tag{9}$$

$$\underline{\boldsymbol{A}}_{L1-3} = \begin{bmatrix} \dfrac{1}{(-0.5 + j\sqrt{3/2})} & 0 \\ 0 & (-0.5 + j\sqrt{3/2}) \end{bmatrix}. \tag{10}$$

Taking into account that the parameters of the input and output filters of both matrix choppers are the same ($L_{F1} = L_{F2} = L_{F3} = L_{F4} = L_F, C_{F1} = C_{F2} = C_{F3} = C_{F4} = C_F, L_{L1} = L_{L2} = L_L$, $C_{L1} = C_{L2} = C_L$), the four terminal parameters (chain parameters) of the input and output filters

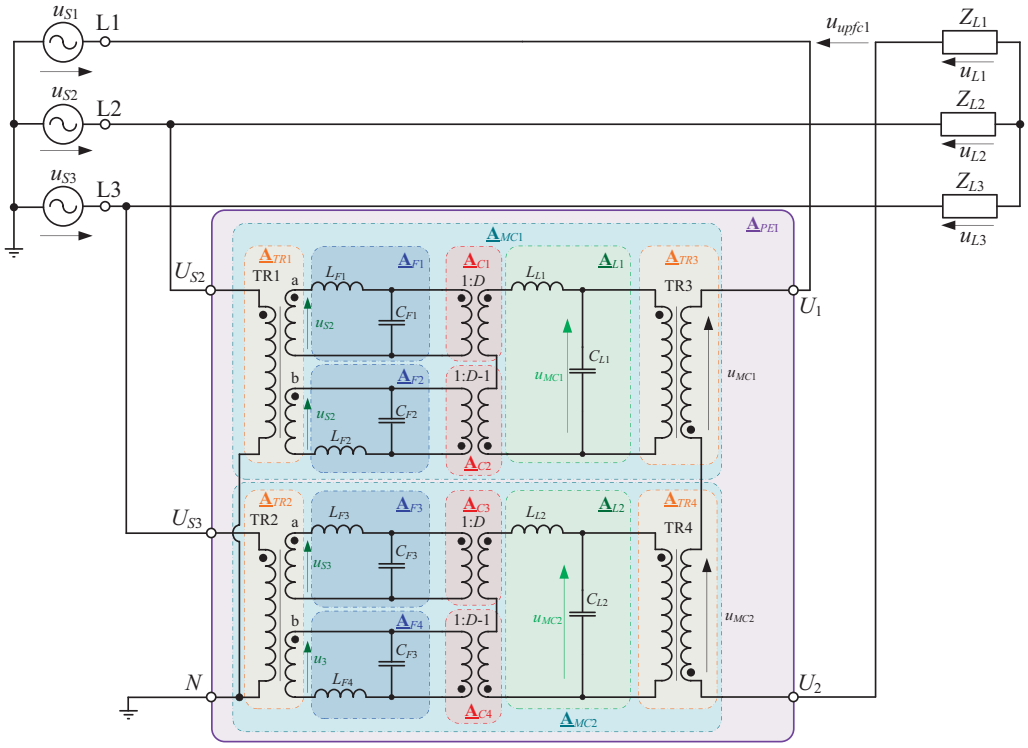

Fig. 6. Averaged circuit model of considered power flow controller based on bipolar direct AC/AC converters

can be described as (11) and (12) respectively. The four terminal parameters of the averaged circuit model of the matrix choppers used are described as (13)–(16) [21].

$$\underline{\boldsymbol{A}}_{\boldsymbol{F}} = \begin{bmatrix} 1 - \omega^2 L_F C_F & j\omega L_F \\ j\omega C_F & 1 \end{bmatrix}, \tag{11}$$

$$\underline{\boldsymbol{A}}_{\boldsymbol{L}} = \begin{bmatrix} 1 - \omega^2 L_L C_L & j\omega L_L \\ j\omega C_L & 1 \end{bmatrix}, \tag{12}$$

$$\underline{\boldsymbol{A}}_{C1} = \begin{bmatrix} \dfrac{1}{D_1} & 0 \\ 0 & D_1 \end{bmatrix}, \tag{13}$$

$$\underline{\boldsymbol{A}}_{C2} = \begin{bmatrix} \dfrac{1}{D_1 - 1} & 0 \\ 0 & D_1 - 1 \end{bmatrix}, \tag{14}$$

$$\underline{\boldsymbol{A}}_{C3} = \begin{bmatrix} \dfrac{1}{D_2} & 0 \\ 0 & D_2 \end{bmatrix}, \tag{15}$$

$$\underline{\boldsymbol{A}}_{C3} = \begin{bmatrix} \dfrac{1}{D_2 - 1} & 0 \\ 0 & D_2 - 1 \end{bmatrix}. \tag{16}$$

Taking into account that the voltage ratios of transformers *TR*1–*TR*4 are assumed as 1:1, the chain parameters of input (*TR*1, *TR*2) and output (*TR*3, *TR*4) transformers can be described as (17) and (18), respectively.

$$\underline{\boldsymbol{A}}_{TR1a} = \underline{\boldsymbol{A}}_{TR1b} = \underline{\boldsymbol{A}}_{TR2a} = \underline{\boldsymbol{A}}_{TR2b} = \begin{bmatrix} 1 & 0 \\ 0 & 1 \end{bmatrix}, \tag{17}$$

$$\underline{\boldsymbol{A}}_{TR3} = \underline{\boldsymbol{A}}_{TR4} = \begin{bmatrix} 1 & 0 \\ 0 & 1 \end{bmatrix}. \tag{18}$$

In accordance with four-terminal theory [22] and taking into account the type of connections of the four terminal networks, we can easily obtain substitute chain parameters of the analysed circuit. Moreover, to obtain a four-terminal description of the considered power flow controller it is necessary to introduce a matrix of chain parameters of source voltage $\underline{\boldsymbol{A}}_{US1}$ (19) connected in series with the load and output of power electronic module PE I (Fig. 7).

$$\underline{\boldsymbol{A}}_{US1} = \begin{bmatrix} 1 & 0 \\ 0 & 1 \end{bmatrix}, \tag{19}$$

Applying the four-terminal description method [22] and the procedure described in Fig. 7 it is easily to obtain the four terminal parameters of the considered circuit (20), where *G* represents four-terminal hybrid parameters.

$$\begin{bmatrix} \underline{U}_{S1} \\ \underline{I}_{S1} \end{bmatrix} = \underline{\boldsymbol{A}}_I \begin{bmatrix} \underline{U}_{L1} \\ \underline{I}_{L1} \end{bmatrix} = \begin{bmatrix} \underline{A}_{I\_11} & \underline{A}_{I\_12} \\ \underline{A}_{I\_21} & \underline{A}_{I\_22} \end{bmatrix} \begin{bmatrix} \underline{U}_{L1} \\ \underline{I}_{L1} \end{bmatrix} = \frac{1}{\underline{G}_{I\_21}} \begin{bmatrix} 1 & -\underline{G}_{I\_22} \\ \underline{G}_{I\_11} & -\det \underline{\boldsymbol{G}}_I \end{bmatrix} \begin{bmatrix} \underline{U}_{S1} \\ \underline{I}_{L1} \end{bmatrix}. \tag{20}$$

In accordance with four-terminal theory [22], we obtain dependences on voltage transmittance (21) and phase of voltage transmittance (22) of the considered circuit.

$$\underline{H}_U = \frac{\underline{U}_{L1}}{\underline{U}_{S1}} = \frac{1}{\underline{A}_{I\_11} + \underline{A}_{I\_12}/Z_{L1}}, \tag{21}$$

$$\arg \underline{H}_U = \arg\left(\frac{1}{\underline{A}_{I\_11} + \underline{A}_{I\_12}/Z_{L1}}\right). \tag{22}$$

Graphical interpretations of dependencies (21) and (22) are shown in Fig. 8(a) and 8(b), respectively.

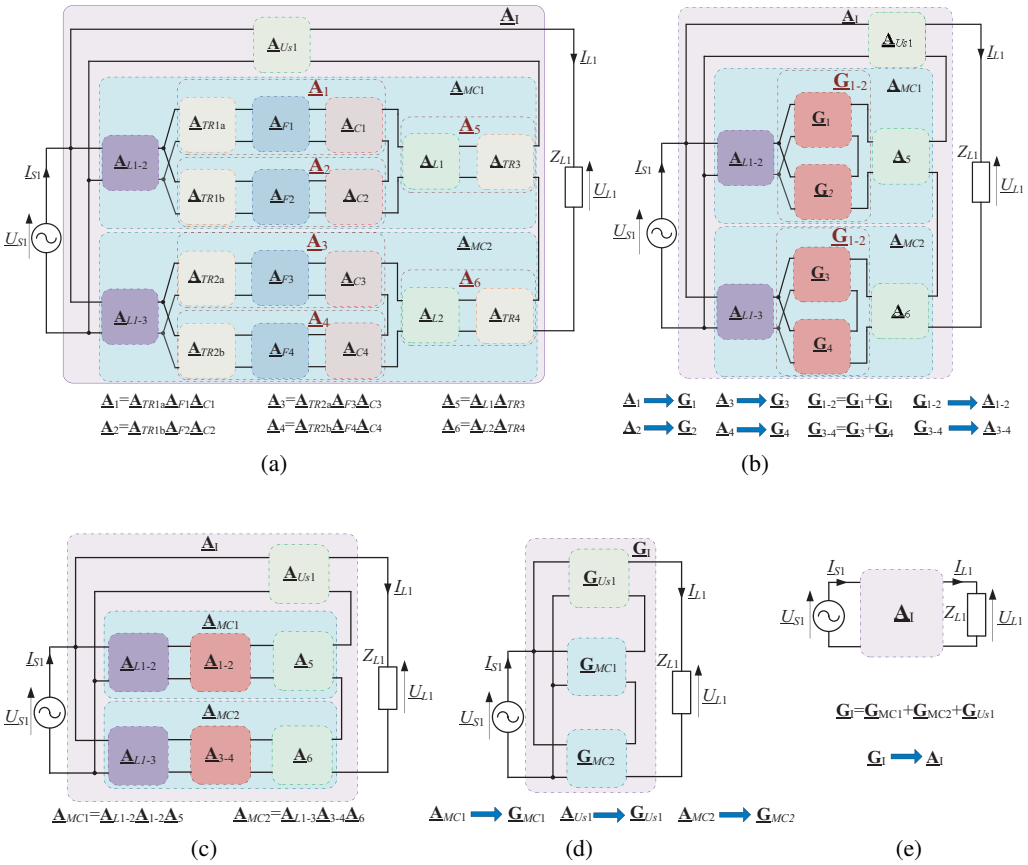

Fig. 7. Equivalent schematic diagram of considered power flow controller and its subsequent transformations: (a) main circuit; (b) after first transformation; (c) after second transformation; (d) after third transformation; (e) substitute final four-terminal network

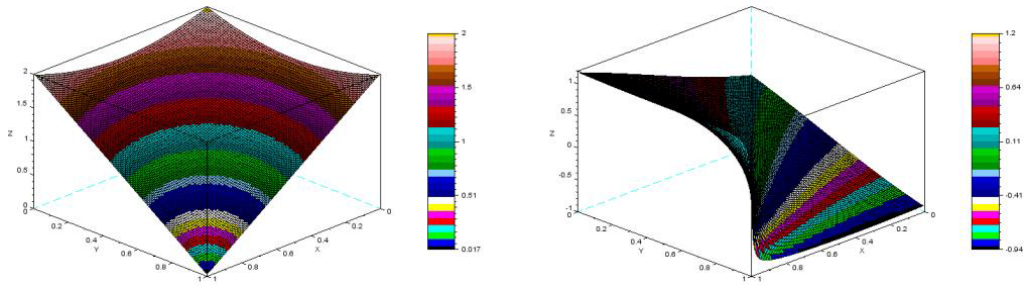

Fig. 8. Characteristics as a function of duty factors D_1 and D_2: (a) voltage transmittance; (b) phase of voltage transmittance

Voltage transmittance H_U (also called voltage gain) can be changed in the range from 0 to $2U_S$. This means that the considered circuit has a buck-boost character and that the output voltage can be lower or higher than source voltage U_S, depending on pulse duty factors D_1 and D_2 (Fig. 8(a)). Also, the phase of the output voltage can by changed, depending on pulse duty factors D_1 and D_2 (Fig. 8(b)). The range of change of the output voltage phase is approximately ±60°. These properties give the opportunity to control and compensate overvoltages and voltage sags up to 50% of U_S, and deal with single phase interruption and power flow control in the AC power system.

4. Experimental results

The schematic diagram and photo of the experimental set of the analyzed power flow controller are shown in Fig. 9. The parameters of the experimental set were as follows: rated power $S = 1$ kVA, supply and load voltage $U_S = 100$ V, $U_L = 100$ V respectively, inductance and capacitance of input/output LC filters $L_F = L_L = 1$ mH, $C_F = C_L = 20$ µF, line reactance $X_L = 30\,\Omega$, switching frequency $f_s = 10$ kHz, which is a compromise between commutation losses, conducting losses and the size of passive LC filters.

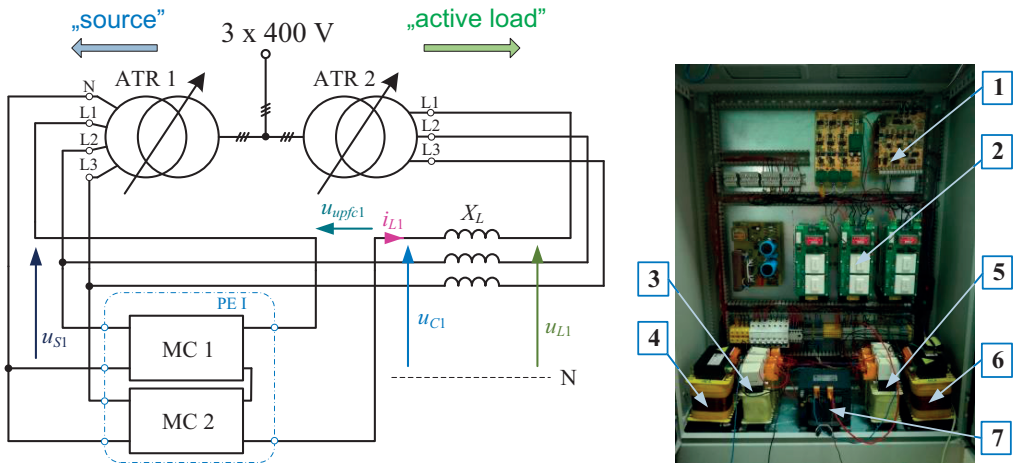

(a) (b)

Fig. 9. Experimental set: (a) schematic; (b) photo: 1 – PWM control circuit, 2 – matrix chopper, 3, 5 – input/output LC filters, 4, 6 – input transformers, 7 – output transformer

The voltage phasors and experimental time waveforms of voltages, currents and instantaneous power for various conditions are shown in Fig. 10. All cases are shown for equal values of the rms voltage of the source (U_S), load (U_L) and output voltage of the power flow controller (U_{C1}).

In the condition when the source voltages (u_S), load voltages (u_L) and output voltage of the power flow controller (u_{C1}) are the same (Fig. 10(a)) there is no energy exchange between the sources (no power flow). In the case when voltage $\underline{U}_{C1}$ is delayed in the phase in relation

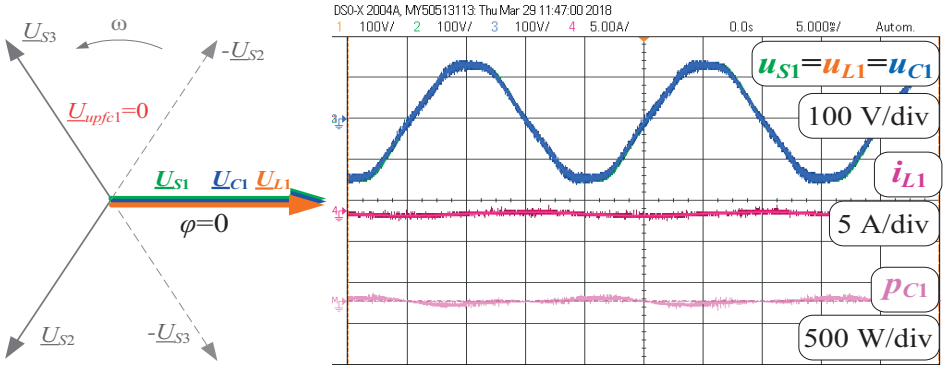

(a)

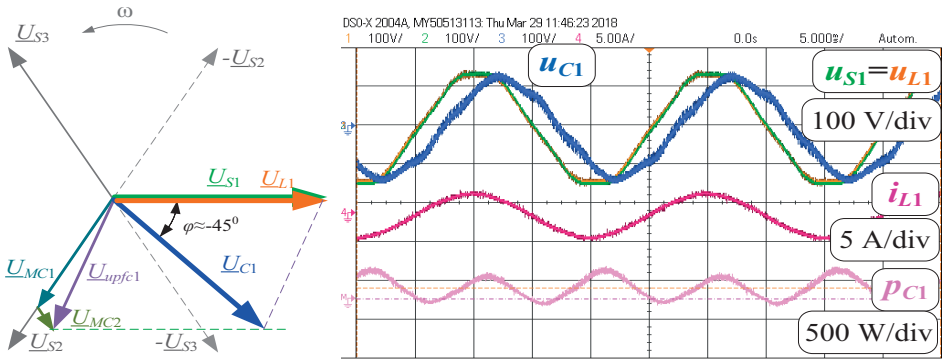

(b)

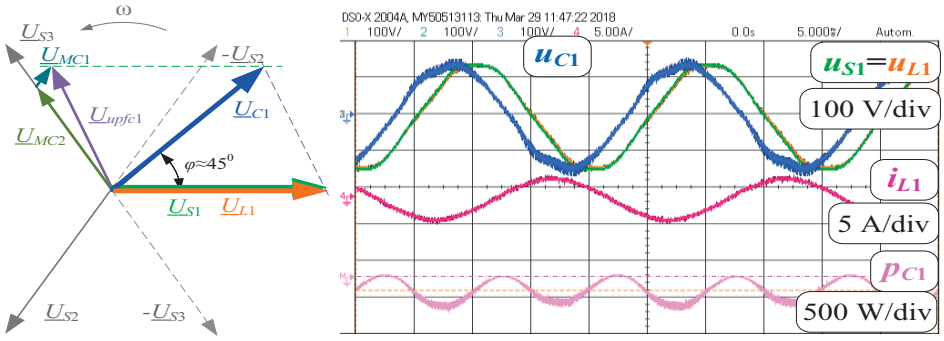

(c)

Fig. 10. Experimental voltage phasors and voltage, current and instantaneous power time waveforms at conditions: (a) $u_{S1} = u_{L1} = u_{C1}$, $U_{S1} = U_{L1} = U_{C1}$, $\varphi \approx 0$; (b) $u_{S1} = u_{L1}$, $U_{S1} = U_{L1} = U_{C1}$, $\varphi \approx -45°$; (c) $u_{S1} = u_{L1}$, $U_{S1} = U_{L1} = U_{C1}$, 45°

to voltage $\underline{U}_{L1}$ (Fig. 10(b)) the instantaneous power (p_{C1}) is positive, which means that energy is transferred to the load. The opposite is the case if voltage $\underline{U}_{C1}$ is ahead of voltage $\underline{U}_{L1}$ (Fig. 10(c)). In addition, the amplitude of the output voltage of the power flow controller can be changed (Fig. 11).

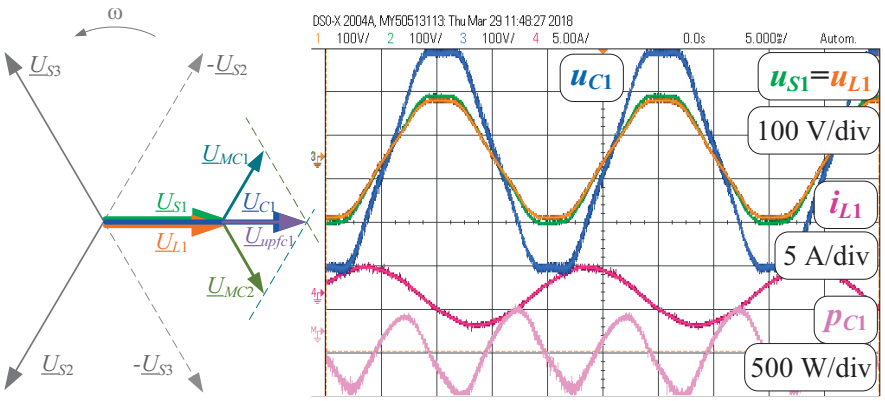

(a)

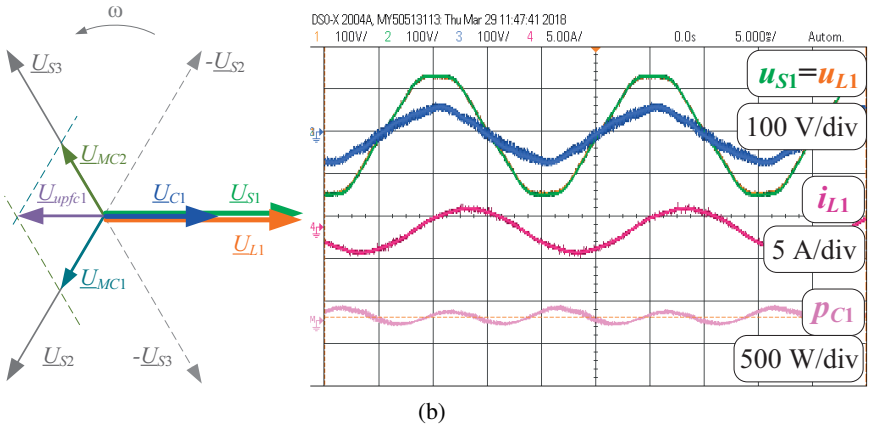

(b)

Fig. 11. Experimental voltage phasors and voltage, current and instantaneous power time waveforms under conditions: (a) $u_{S1} = u_{L1}$, $U_{S1} = U_{L1}$, $\varphi \approx 0$, $U_{C1} > U_{S1}$; (b) $u_{S1} = u_{L1}$, $U_{S1} = U_{L1}$, $\varphi \approx 0$, $U_{C1} < U_{S1}$

As alredy mentioned, to control only the voltage amplitude, both pulse duty factors must have the same value ($D_1 = D_2$). If both duty factors are equal and lower than 0.5, voltage $\underline{U}_{C1}$ is higher than source voltage $\underline{U}_{S1}$ (Fig. 11(a)). If the pulse duty factors are higher than 0.5, voltage $\underline{U}_{C1}$ is lower than source voltage $\underline{U}_{S1}$ (Fig. 11(b)). The source side current and active load side current, for various operating conditions are shown in Fig. 12 (during the control of the voltage phase (Fig. 12(a)), during the control of the voltage amplitude (Fig. 12(b)). Because the presented power flow is a kind of series device, the grid side current and active load side current are similar.

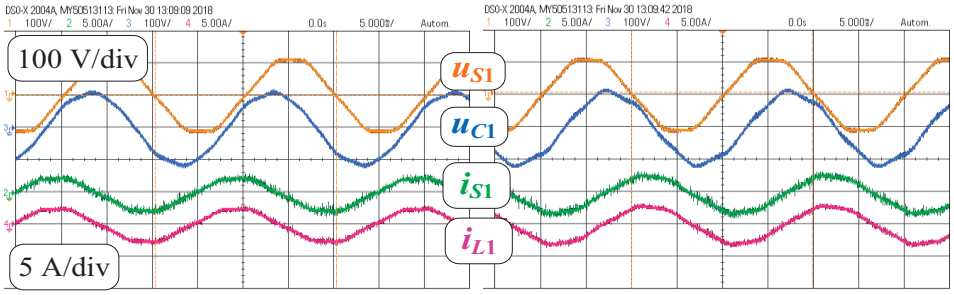

(a)

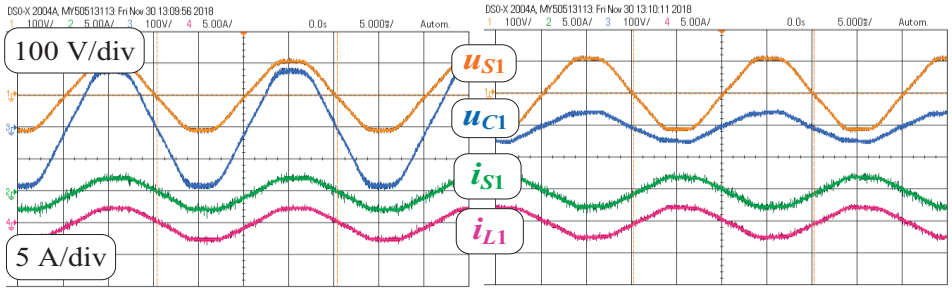

(b)

Fig. 12. Experimental voltages and currents time waveforms: (a) phase control; (b) amplitude control

5. Conclusions

A three phase power flow controller with direct PWM AC/AC converters, for the control of amplitude and phase of voltage, is presented in this paper. The main circuit and operation principle have been described. The article presents a theoretical analysis based on the average circuit model of the considered power flow controller, obtained on the basis of averaged state variables and the four-terminal description method. On the basis of theoretical analysis the static characteristics of magnitude and the phase of voltage transmittance have been obtained. The experimental laboratory model was built for a rated power of 1 kVA. For power flow analysis, the experimental research was carried out with an active load (in a two-source system). Considering the main properties and the characteristic way of supplying the power electronic modules in particular phases, the analyzed circuit has the ability to compensate 50% three-phase voltage sag/swell and single phase voltage interruption. Additionally, by voltage phase control (approximately with in ±60° in each phase) it is possible to control the power flow in the AC power system. The construction of the AC/AC bipolar converter used is quite simple, but it requires a transformer with a center tap. Moreover, control signals for each of the AC/AC converters are easy to obtain and are based on the conventional PWM control method. The next step of the investigation will be focused on the implementation of a control system with a closed control loop and analysis of the dynamic properties.

References

[1] Slootweg J.G., Kling. W.L., *The impact of large scale wind power generation on power system oscillations*, Electric Power Systems Research, vol. 67, pp. 11–20 (2003).

[2] Mehta B., Bhatt P., Pandya V., *Small signal stability analysis of power systems with DFIG based wind power penetration*, International Journal of Electrical Power & Energy Systems, vol. 58, pp. 64–74 (2014).

[3] Milanovic J.V., *Characteristics of voltage sags in radial networks with dynamic loads and embedded generators*, Power Tech Proceedings, Porto, vol. 1 (2001).

[4] Iravani M.R., Maratukulam D., *Review of Semiconductor-Controlled (STATIC) Phase Shifters for Power System Applications*, IEEE Transactions on Power Systems, vol. 9, no. 4, pp. 1833–1839, November (1994).

[5] Lopes L.A.C., Joos G., Ooi B.T., *A PWM Quadrature Booster Phase-Shifter for FACTS*, IEEE Transactions on Power Delivery, vol. 11, no. 4, pp. 1999–2004, October (1996).

[6] Kaniewski J., Fedyczak Z., *Modelling and Analysis of a Three-Phase Quadrature Phase Shifter with a Hybrid Transformer*, Przegląd Elektrotechniczny, no. 11, pp. 269–274 (2008).

[7] Shuitao Yang, Yang Liu, Xiaorui Wang, Deepak Gunasekaran, Ujjwal Karki, Fang Z. Peng, *Modulation and Control of Transformerless UPFC*, IEEE Transactions on Power Electronics, vol. 31, iss. 2, pp. 1050–1063, February (2016).

[8] Jiaxin Yuan, Lei Liu, Wenli Fei, Li Chen, Baichao Chen, Bo Chen, *Hybrid Electromagnetic Unified Power Flow Controller: A Novel Flexible and Effective Approach to Control Power Flow*, IEEE Transactions on Power Delivery, vol. 33, iss. 5, pp. 2061–2069, October (2018).

[9] Monteiro J., Fernando Silva J., Pinto S.F., Palma J., *Linear and Sliding-Mode Control Design for Matrix Converter-Based Unified Power Flow Controllers*, IEEE Trans on Power Electronics, vol. 29, no. 7, pp. 3357–3367, July (2014).

[10] Monteiro J., Fernando Silva J., Pinto S.F, Palma J., *Matrix Converter-Based Unified Power-Flow Controllers: Advanced Direct Power Control Method*, IEEE Trans. on Power Delivery, vol. 26, no. 1, pp. 420–430, January (2011).

[11] Kaniewski J., Szcześniak P., Jarnut M., Fedyczak Z., *Voltage conditioner & power flow controller based on bipolar matrix-reactance choppers*, Electrical Power and Energy Systems, vol. 94, pp. 256–266 (2018).

[12] Szcześniak P., *Three-phase AC–AC power converters based on matrix converter topology. Matrix-reactance frequency converters concept*, Berlin-Heidrberg, Springer (2013).

[13] Friedli T., Kolar J.W., Rodriguez J., Wheeler P.W., *Comparative evaluation of threephase AC–AC matrix converter and voltage DC-link back-to-back converter systems*, IEEE Transactions on Industrial Electronics, vol. 59, no. 12, pp. 4487–510 (2011).

[14] Babaei E., Farhadi Kangarlu M., *Sensitive load voltage compensation against voltage sags/swells and harmonics in the grid voltage and limit downstream fault currents using DVR*, Electr. Power Syst. Res., vol. 83, pp. 80–90 (2012).

[15] Kaniewski J., *Hybrid distribution transformer based on a bipolar direct AC/AC converter*, IET Electric Power Applications, vol. 12, iss. 7, pp. 1034–1039, August (2018)

[16] Oliveira J.C., Freitas L.C., Coelho E.A.A., Farias V.J., Viaira Jr. J.B., *A PWM AC/AC Full-Bridge used like a Shunt and serial Regulator*, Proc. European Conf. on Power Electr. and Applic., Trondheim, pp. 2.186–2.191 (1997).

[17] Middlebrock R.D., Ćuk S., *General unified approach to modeling switching converter power stages*, in Rec. IEEE PESC 76, pp. 18–34 (1976).

[18] Fedyczak Z., *Steady state modelling of the bipolar PWM AC line matrix-reactance choppers based on Ćuk topologies*, Archives of Electrical Engineering, vol. 62, no. 3, pp. 303–316 (2003).

[19] Fedyczak Z., Frąckowiak L., Jankowski M., *A serial AC voltage controller using bipolar matrix-reactance chopper*, COMPEL – The International Journal for Computation and Mathematics in Electrical and Electronic Engineering, vol. 25, no. 1, pp. 244–258 (2006).

[20] Kaniewski J., Fedyczak Z., Benysek G., *AC voltage sag/swell compensator based on three-phase hybrid transformer with buck-boost matrix-reactance chopper*, IEEE Trans. Ind. Electron., vol. 61, no. 8, pp. 3835–3846, August (2014).

[21] Kaniewski J., Jarnut M., Szcześniak P., Fedyczak Z., *The study of smart distribution transformer based on a bipolar matrix chopper*, Proc. Compatibility, Power Electronics and Power Engineering, Cadiz, Spain, April (2017).

[22] David Irwin J., Nelms R. M., *Basic Engineering Circuit Analysis*, 10th Ed, WILEY John Wiley & Sons, Inc. (2011).

[23] Kaniewski J., *Three-Phase Power Flow Controler Based on Bipolar AC/AC Converter with Matrix Choppers*, International Symposium on Power Electronics, Electrical Drives, Automation and Motion – SPEEDAM 2018, Amalfi Coast, Italia (2018).